Research on an energy model for X-ray measurement of paper ash content using COMSOL

LIANHUA HU AND WENBO CHEN

ABSTRACT: Ash content is one of the critical quality parameters in papermaking production. Traditional ^{55}Fe radioactive sources used for online ash content measurement have a short lifespan and high costs, while offline methods such as the combustion method or chemical analysis are time-consuming. Using an X-ray tube as the radiation source, continuous X-ray measurement offers advantages such as being rapid, non-destructive, and cost-effective.

In this study, COMSOL software was employed to simulate the measurement process and establish an energy attenuation model for X-ray measurement of paper ash content. The model simulates the energy attenuation of X-rays before and after transmission through four materials: calcium carbonate ($CaCO_3$), titanium dioxide (TiO_2), wood-based plant fibers, and paper samples filled with $CaCO_3$. The absorption coefficients of paper samples with varying ash content were investigated using the model and compared with experimental results obtained from continuous X-ray measurements. The results indicate that the proposed energy simulation model can reduce the measurement error of paper ash content by 1%, significantly enhancing the reliability and accuracy of ash content measurement.

Application: This study focuses on continuous X-ray measurement of paper ash content. Using COMSOL software, we simulated the measurement process and developed an X-ray energy attenuation simulation model for measuring paper ash content. The reliability and accuracy of ash content measurement were significantly improved.

The ash content of paper is closely related to its physical properties such as smoothness, whiteness, and opacity. Therefore, accurately determining the ash content of paper is a crucial aspect of paper quality control [1-3]. In recent years, research on paper ash content has deepened, with the primary ray detection methods including X-ray fluorescence, X-ray diffraction, and energy-dispersive X-ray fluorescence (EDXRF) [4]. The X-ray fluorescence method proposed by Huang [5], based on the selective absorption characteristics of paper, can achieve high-precision measurements within 30 s, with a measurement error of less than 1% and a root mean square error of ±0.58%. Ou [6] and others used ^{55}Fe isotopes as a radiation source to study the absorption relationship between soft X-rays and paper ash content. Rozic [7] and others employed EDXRF technology for elemental analysis of paper, further expanding the scope of ash content research. Traditional ^{55}Fe radiation source methods suffer from the drawbacks of high cost and short lifespan. Lu [8] proposed a continuous X-ray method using an X-ray tube for the quantitative detection of total ash content and its components in paper. This approach offers lower costs and shorter measurement times.

The X-rays emitted by the ^{55}Fe radiation source are concentrated at 5.9 keV, while the X-rays generated by the X-ray tube have an energy range from 100 eV to 100 keV, with a continuous wavelength spectrum between 0.01 nm and 10 nm. Therefore, when using continuous X-rays from an X-ray tube to measure paper ash content, the absorption coefficients of different fillers for the continuous X-rays are key factors affecting measurement accuracy. Many researchers have utilized the Monte Carlo N-Particle (MCNP) program to calculate the energy absorption coefficients of media for X-rays of different energies [9] and employed the Monte Carlo algorithm to study the characteristics of X-rays [10-16]. Finite element methods have also been used to model X-ray tubes, investigating their performance under various working conditions and optimizing X-ray tube design [17-19].

This study uses the COMSOL software finite element method (COMSOL; Burlington, MA, USA) to simulate the process of continuous X-ray detection for paper ash content, establishing an energy simulation model for X-ray measurement. The interaction between X-rays and paper is modeled to gain a deeper understanding of the energy transformation of X-rays within the paper. By integrating experimental results with simulation data, the absorption coefficients of continuous X-rays in paper with varying filler contents are analyzed. This research aims to further enhance the reliability and accuracy of paper ash content measurement.

PRINCIPLE OF CONTINUOUS X-RAY MEASUREMENT OF PAPER ASH CONTENT

X-ray tube and X-ray energy calculation

In an X-ray tube, when high-speed electrons collide with the metal cathode target, their abrupt deceleration converts kinetic energy into electromagnetic radiation, producing X-rays through Bremsstrahlung. The intensity of rays generated by the X-ray tube is related to factors such as the energy of the electron, the atomic number of the target material, and the impact angle [20].

The relationship between the limit short wavelength of the Bremsstrahlung continuum spectrum of X-ray tubes and the tube voltage is:

$$\lambda_{min} = 124/V \quad (1)$$

The relationship between the maximum intensity wavelength and the ultimate short wavelength of the Bremsstrahlung continuum spectrum of X-ray tubes is:

$$\lambda_{max} = 1.5\lambda_{min} \quad (2)$$

The relationship between the average wavelength of the Bremsstrahlung continuum spectrum of X-ray tubes and the extreme short wavelength is:

$$\lambda_{mean} = 2.5\lambda_{min} \quad (3)$$

The relationship between the total energy intensity of the X-ray tube and tube voltage, tube current, and atomic number is:

$$l_0 = kiZV^2 \quad (4)$$

In the previous equations, λ_{min} is the shortwave limit wavelength of the X-ray continuous spectrum (nm); λ_{max} is the wavelength corresponding to the maximum intensity of the continuous X-ray spectrum (nm); λ_{mean} is the short average wavelength of the X-ray continuum spectrum (nm); l_0 is the incident intensity of continuous spectrum rays; k is the proportional coefficient, i is the tube current (mA); V is the tube voltage (kV); and Z is the atomic number of the ray tube target.

Scattering attenuation phenomenon of X-rays passing through paper

When X-rays penetrate a certain thickness of material, they undergo a series of complex interactions with the material. The interactions between X-rays and matter occur in several ways, primarily including the photoelectric effect, coherent scattering (Rayleigh scattering), incoherent scattering (Compton effect), and pair production. For low-energy X-rays and materials with high atomic numbers, the photoelectric effect predominates. For medium-energy X-rays and materials with high atomic numbers, the Compton effect dominates, while for high-energy X-rays and materials with high atomic numbers, pair production is the dominant interaction [21,22].

When X-rays pass through a material, the bound electrons in the target material's atoms undergo inelastic collisions with the X-rays, resulting in the ejection of electrons. This process causes the X-rays to lose energy and change direction, known as Compton scattering. Interactions between X-rays and matter may lead to energy loss, while X-rays that do not interact continue to penetrate the material. The probability of photon interactions with matter is described by the theoretical value of the photon interaction cross-section, σ_{tot}, which represents the probability of photon-atom interactions per unit area. The total interaction cross-section is the sum of its individual components [23]:

$$\sigma_{tot} = \sigma_{pe} + \sigma_{coh} + \sigma_{incoh} + \sigma_{pair} + \sigma_{trip} \quad (5)$$

where σ_{pe} is the photoelectric effect cross-section; σ_{coh} and σ_{incoh} are the coherent (Rayleigh) and incoherent (Compton) scattering cross-sections, respectively; and σ_{pair} and σ_{trip} are the electron pair cross-sections in the atomic nucleus and atomic electron fields, respectively.

The linear attenuation coefficient μ represents the total probability of interaction between X-rays and matter such as photoelectric effect, Compton effect, and electron pair generation at unit distance (cm^{-1}). For a given material, the relationship between σ_{tot} and μ is:

$$\mu = N \bullet \sigma_{tot} \quad (6)$$

where N is the atomic number density of the material.

When the X-rays emitted by the X-ray tube penetrate the paper, its energy intensity complies with Beer's attenuation law [24]. A narrow beam of monoenergetic photons with incident intensity I_0 penetrates a sample with mass thickness x and density ρ. The changes in X-ray energy intensity are as follows:

$$I = I_0 e^{-(\mu/\rho)x} \quad (7)$$

where I is the X-ray intensity after penetrating the paper; μ/ρ is the mass attenuation coefficient of the sample to X-rays (cm^2/g); and x is the basis weight (g/cm^2), defined as the mass per unit area.

COMSOL model parameter settings

This study employs the bidirectional coupling ray tracing module of COMSOL software to simulate the process of using continuous X-rays to detect paper ash content. A simulation model for measuring the energy of paper and ash content was established to investigate the energy variation during the interaction between X-rays and paper. As X-rays penetrate the medium and air domains, intensity attenuation occurs. By calculating the intensity changes before and after attenuation and incorporating parameters such as the material's attenuation coefficient, density, and thickness, the ash content in the model can be determined.

In the geometry module, three rectangles of incident air, transmitted air, and paper ash model are set as the research domain. At the ray emission end, the upper boundary of the incident air domain is used as the ray release boundary, and the experiment simulates the continuous X-rays generated by the X-ray tube voltage and current of 10000 V and 0.28 mA, respectively. The maximum energy of the ray is set to 10 keV; the energy spectrum of the ray tube is evenly distributed; and the release mode is uniformly distributed.

At the ray receiving end, the lower boundary of the transmitted air domain is used as the detector. In order to improve the consistency between the simulation and experimental data, the receiving mode is set to Poisson distribution to simulate the randomness of the arrival of photons, and the counting process of each photon is simulated.

The material properties of the study domain are set as attenuation coefficient, refractive index, material density, and reference temperature and pressure, respectively. The mass attenuation coefficients of photons acting with various materials can be queried by the international standard NIST database [25]. The mass attenuation coefficients of X-rays in compounds or mixtures can be calculated according to Eq. 8:

$$\mu/\rho = \sum_i (W_i \bullet \mu_i/\rho_i) \tag{8}$$

where ρ is the density of the compound, μ_i/ρ_i is the mass decay coefficient of each constituent element of the compound, and W_i is the mass percentage of the element.

There is a certain correlation between the refractive index of the material and the wavelength, and the refractive index of the material may be slightly different depending on the wavelength, so the optical dispersion model is set up in the simulation. Dispersion phenomenon means that light of different wavelengths will propagate at different speeds in the same material, resulting in light deflection and dispersion effects [26]. Sellmeier's formula describes the relationship between the refractive index of a material and its wavelength, and it is usually used to describe the optical properties of non-metallic materials. The general form of Sellmeier's formula is shown in Eq. 9:

$$n(\lambda) = \sqrt{1 + \sum_j \frac{A_j \lambda^2}{\lambda^2 - B_j}} \tag{9}$$

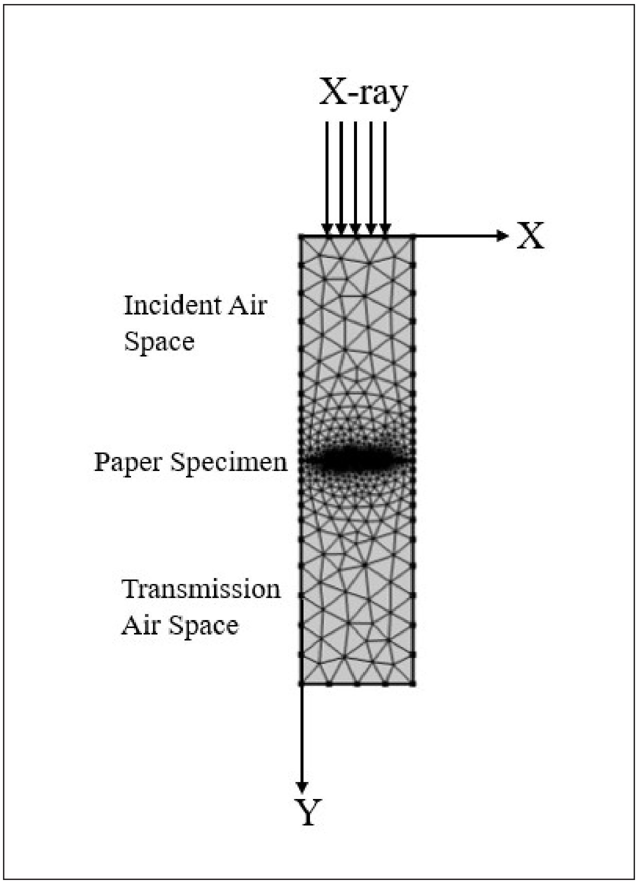

1. Schematic of COMSOL simulation model.

where $n(\lambda)$ is the refractive index; λ is the wavelength; and A_j and B_j are Sellmeier coefficients, which are empirical coefficients fitted from experimental data.

The sample measurement model has dimensions of 10 mm × 0.08 mm in the X and Y directions, with the X-ray beam incident perpendicular to the X-axis on the material surface. The cross-sectional area of the X-ray beam in the XY direction is much smaller than the area of the irradiated material in the XY direction. For each condition, 100 ray trajectories are traced in the calculation. To eliminate statistical errors caused by the finite number of ray trajectories, as well as minor errors due to the physical model and numerical calculations, the calculation results are ensured to have an error within 2%. The geometric structure of the COMSOL ray tracing simulation model for paper ash content measurement established in this study is shown in **Fig. 1**.

The main objects of this study are office paper and newsprint. Therefore, the energy attenuation of continuous X-rays at 10 keV was calculated in the four materials: calcium carbonate ($CaCO_3$), titanium dioxide (TiO_2), poplar wood plant fibers, and $CaCO_3$-filled paper samples. Using Eq. 7 and Eq. 8 along with the mass attenuation coefficient data of the relevant materials [25], the energy attenuation of X-rays passing through $CaCO_3$, TiO_2, pop-

Materials	$CaCO_3$	TiO_2	Woody Plant Fiber	$CaCO_3$-Filled Paper Sample
Mass attenuation coefficient (μ/ρ), cm²/g	0.3915	0.4554	0.0566	0.1058
Density (ρ), g/cm³	2.9300	4.2600	1.5000	0.7955
$CaCO_3$: calcium carbonate; TiO_2: titanium dioxide.				

I. Densities and mass attenuation coefficients at 10 keV for several materials.

lar wood plant fibers, and $CaCO_3$-filled paper samples was calculated. **Table I** shows the mass attenuation coefficients and densities of these four materials.

ANALYSIS OF SIMULATION MODEL CALCULATION RESULTS

Attenuation of X-rays in paper and its ash materials

The incident air domain has dimensions of 15 mm × 30 mm in the *X* and *Y* directions, while the dimensions of the paper ash material are set to 10 mm × 0.08 mm in the *X* and *Y* directions. The transmitted air domain also has dimensions of 15 mm × 30 mm in the *X* and *Y* directions, with an environmental temperature of 293 K and reference pressure of 101 kPa. In this study, based on Eq. 8 and the mass attenuation coefficient data of the relevant materials, COMSOL was used to calculate the intensity variation of X-rays transmitted through four materials — $CaCO_3$, TiO_2, lignocellulosic fibers, and $CaCO_3$-filled paper samples — as shown by the solid red lines in **Figs. 2–5**. Simultaneously, the energy intensity attenuation of X-rays transmitted through these four different materials was calculated theoretically using Eq. 7 (black dashed lines in Figs. 2–5).

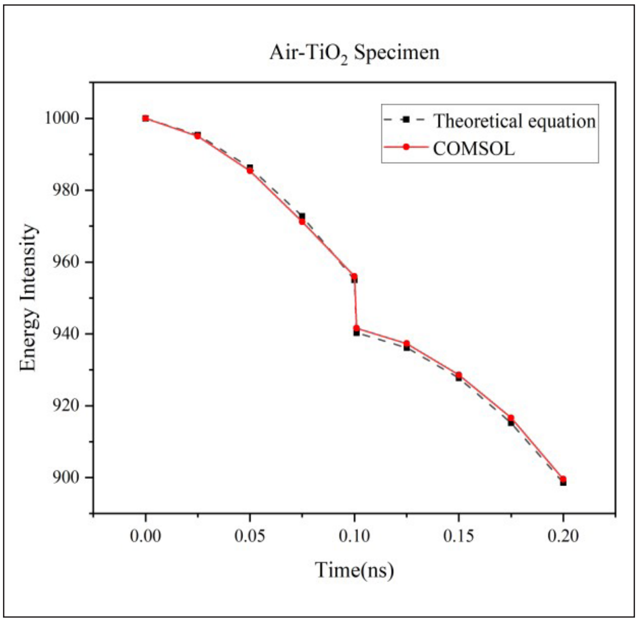

3. Intensity attenuation of X-rays through titanium dioxide (TiO_2) medium.

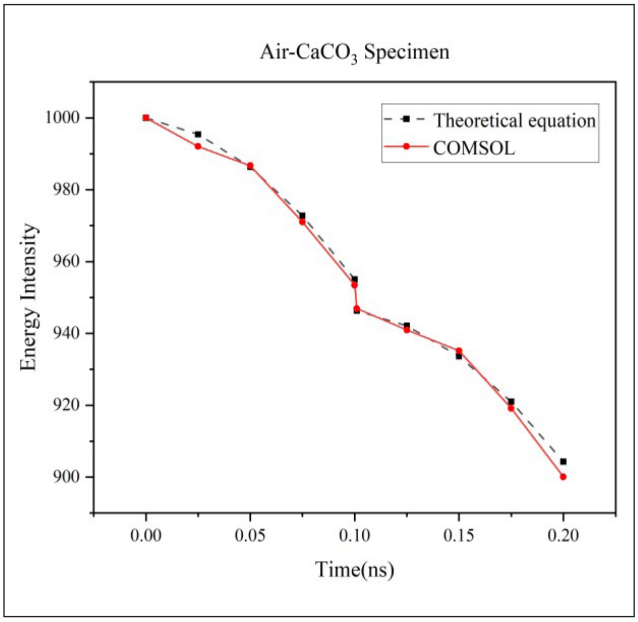

2. Intensity attenuation of X-rays through calcium carbonate ($CaCO_3$) medium.

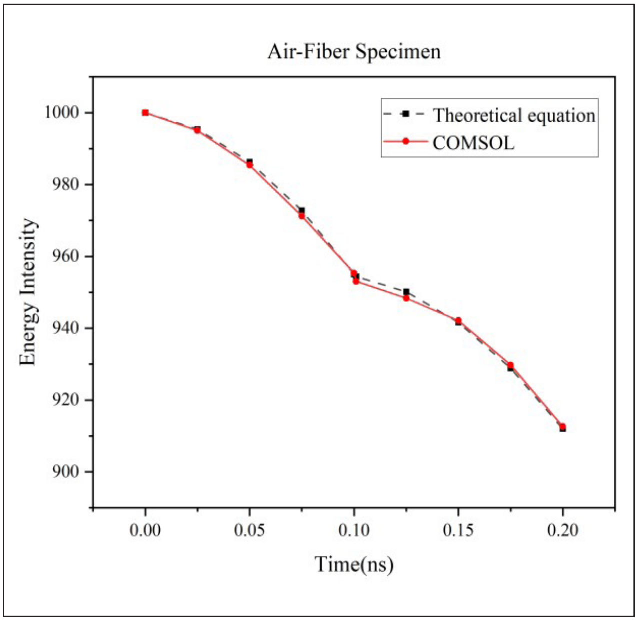

4. Intensity attenuation of X-rays through plant fibers.

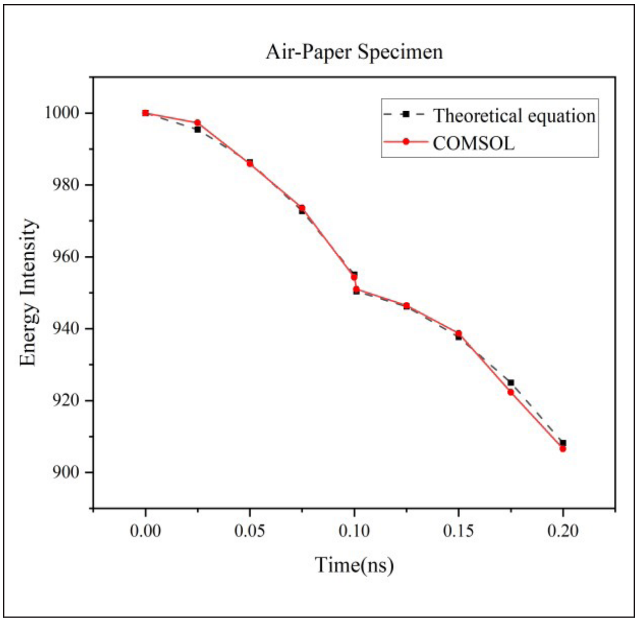

5. Intensity attenuation of X-rays through $CaCO_3$-filled paper.

The theoretical calculation results and the model results have a deviation within 3%. The cause of the error is due to the refraction of X-rays in the medium and the temperature changes induced by the absorption of X-rays in the material. The density and refractive index changes of the air gap affect the ray trajectory, altering the transmission thickness, resulting in incomplete transmission of the X-rays or an increased transmission distance through the material at an angle, which in turn affects the calculation of attenuation intensity.

The COMSOL simulation results show that when X-rays sequentially pass through the incident air domain, the medium, and the transmitted air domain, the X-ray energy intensity is significantly attenuated in a relatively short time in all four different material mediums. The X-rays produce significant attenuation when passing through $CaCO_3$ and TiO_2 (Fig. 2 and Fig. 3, respectively), with the intensity attenuation of the 0.008-cm-thick medium layer approaching 2%, which is 466.25% of the intensity attenuation of the air medium under the same conditions (as shown by the folded line portion before 0.10 ns in Fig. 2). In comparison, TiO_2 causes slightly more attenuation of X-rays than $CaCO_3$. When the X-ray energy is maintained under certain conditions, the atomic number and density of the material affect its ability to absorb and attenuate X-rays. Generally, materials with high atomic numbers and their compounds show stronger absorption and greater attenuation at the same X-ray energy.

When X-rays pass through the plant fiber and $CaCO_3$-filled paper models (Fig. 4 and Fig. 5, respectively), the attenuation of the X-ray energy intensity is smaller compared to $CaCO_3$ and TiO_2. This is because plant fibers and paper are primarily composed of carbon (C), hydrogen (H), and oxygen (O), which have smaller atomic numbers and lower densities, resulting in weaker X-ray absorption and smaller attenuation. The intensity attenuation of pure plant fiber material is slightly less than that of $CaCO_3$-filled paper, because the addition of $CaCO_3$ increases the mass attenuation coefficient of the paper, altering its density, translucency, and other physical properties.

The absorption of X-rays by pure filler materials (Fig. 2 and Fig. 3) is greater than the absorption by paper containing fillers (Fig. 5), which in turn is slightly greater than the absorption by pure plant fiber materials (Fig. 4). From an energy conversion perspective, this confirms the feasibility of using continuous X-rays to measure paper ash content in experiments.

Comparison and analysis of simulation model and experimental measurement data

To further validate the reliability of the simulation method proposed in this study, a comparison was made with the continuous X-ray method for measuring paper ash content proposed by Hu [27]. Paper samples with different ash contents of $CaCO_3$ and kaolin fillers were selected; the mass attenuation coefficient of the samples was calculated using experimental and simulation methods; and the measurement results were compared. The continuous X-ray method uses an X-ray tube as the radiation source and an ionization chamber as the X-ray receiving device. The X-ray receiving device and measurement amplification circuit convert the X-rays before and after attenuation into voltage signals for collection. Taking the logarithm of both sides of Eq. 7, we get:

$$\mu/\rho = \ln(I_0/I)/x \quad (10)$$

Further converting the intensity to a voltage signal, Eq. (10) becomes:

$$\mu/\rho = \ln\left(\frac{V_{air} - V_{background}}{V_{ash} - V_{background}}\right)/x \quad (11)$$

where:

V_{air}: no measurement voltage (V)

V_{ash}: ash measurement voltage (V)

$V_{background}$: ray-free voltage (V)

$\ln\left(\frac{V_{air} - V_{background}}{V_{ash} - V_{background}}\right)$: logarithmic ratio of voltage

The X-ray tube voltage and current for the quantitative determination of paper ash content using the continuous X-ray method were set to 10 kV and 0.28 mA, respectively. The $V_{background}$ was 0.003 V. The experimental environment was maintained at a temperature of 22°C and 66.25% relative humidity (RH). The X-ray incident air distance and the transmitted air distance were both 1 cm. The paper samples with different ash content of $CaCO_3$ and kaolin fillers used

$CaCO_3$ Paper Sample	Thickness (t), cm	Density (ρ), g/cm³	Mass Attenuation Coefficient (μ/ρ), cm²/g	Total Ash %
1	0.0080	0.7955	0.1058	13.7
2	0.0081	0.7825	0.1036	12.2
3	0.0077	0.8162	0.1104	14.9
4	0.0082	0.8209	0.1089	14.5
Kaolin Paper Sample	**Thickness (t), cm**	**Density (ρ), g/cm³**	**Mass Attenuation Coefficient (μ/ρ), cm²/g**	**Total Ash %**
5	0.0080	1.3692	0.0545	5.1
6	0.0082	1.3962	0.0646	15.8
7	0.0080	1.4301	0.0715	22.9
8	0.0079	1.4479	0.0753	27.8

II. Parameters of different paper specimens.

Sample	Experimentally Derived Mass Attenuation Coefficients (μ_s/ρ), cm²/g	Experimental Error, %	Model Calculated Measured Mass Attenuation Coefficients (μ_e/ρ), cm²/g	Simulation Error, %
1	0.1078	1.91	0.1069	1.06
2	0.1064	2.71	0.1053	1.65
3	0.1128	2.17	0.1119	1.36
4	0.1119	2.73	0.1108	1.72
5	0.0555	1.83	0.0550	0.92
6	0.0661	2.32	0.0653	1.08
7	0.0730	2.10	0.0723	1.12
8	0.0767	1.92	0.0762	1.21

III. Comparison of mass attenuation coefficients between the present model and experimental measurements.

in the experiment were obtained from the Key Laboratory of Pulp and Paper Engineering at Shaanxi University of Science and Technology. The ash content was measured using the Burning method, and the mass attenuation coefficient (μ/ρ) was determined by XRD as the true value. The ash content, mass attenuation coefficients, density, and thickness of the samples are shown in **Table II**.

The previous data are brought into the paper ash model constructed in this paper to calculate the energy intensity before and after X-ray transmission, so as to calculate the mass attenuation coefficient μ/ρ measured by the model, and at the same time, the experimental method is used to measure the logarithmic ratio of the voltage and to calculate the mass attenuation coefficient of the paper, μ/ρ. The results of the simulation calculations are compared with the results of the experimental measurements, as shown in **Table III**.

The logarithmic ratio of the intensity before and after the energy attenuation of the rays obtained from the simulation was calculated, as well as the logarithmic ratio of the voltage obtained from the continuous X-ray method for quantitative paper ash content measurement. Both of these are representations of the energy attenuation occurring as X-rays pass through the paper sample, i.e., the rate of energy change before and after X-ray transmission through the paper. Therefore, they can serve as a basis for

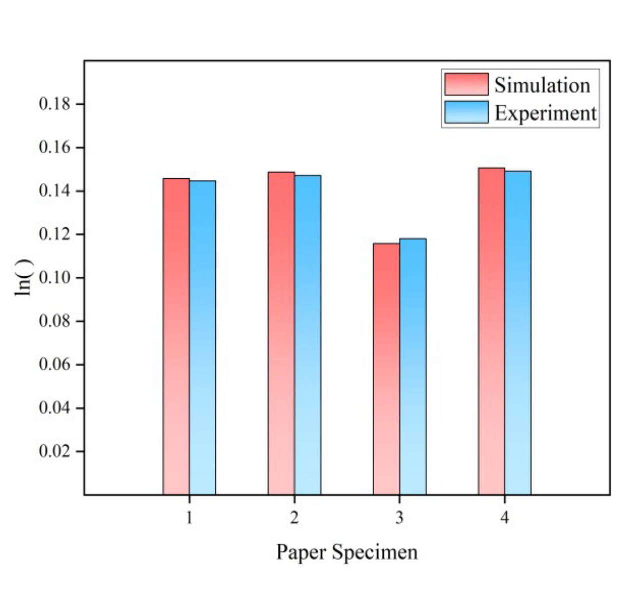

6. Logarithmic ratio of energy intensity vs. logarithmic ratio of voltage.

verifying the similarity between the model and the experiment. The measurement data of the $CaCO_3$ paper sample were used for comparison, and the comparison results are shown in **Fig. 6**.

The experimental results show that the simulation method proposed in this study is in good agreement with the quantitative paper ash content measurements obtained using continuous X-ray measurements. The energy logarithmic ratio calculated by the simulation method is slightly smaller than the voltage logarithmic ratio obtained from experimental measurements, indicating that the rate of energy change after X-ray transmission through the paper is higher in the experimental measurements than in the simulation. This discrepancy is attributed to the influence of environmental factors, equipment operating conditions, and the experimental process on the measured results. The model's calculated results are closer to the true values, with an error of approximately 1% compared to the experimental measurements. This further demonstrates that the simulation model proposed in this study can effectively calculate the mass attenuation coefficient of the sample to be tested.

By inputting the experimental data into the model, the energy intensity change data before and after X-ray transmission through the paper is obtained. Using Eq. 10, the logarithmic ratio of energy intensity is found to be linearly related to the material's mass attenuation coefficient. Assuming the paper composition consists of fibers and ash content, mathematical models for the paper, fiber, and ash are established separately. By solving these models simultaneously, the relationship between the energy intensity logarithmic ratio and the mass attenuation coefficient for ash content in the paper is obtained. The mathematical model is as follows:

$$\ln\left(I_0/I\right) = (\mu_1/\rho)x_1 - (\mu_2/\rho)x_1 + (\mu_2/\rho)x \tag{12}$$

where:
(μ_1/ρ): mass attenuation coefficient of ash to X-ray (cm^2/g)
(μ_2/ρ): mass attenuation coefficient of fiber to X-ray (cm^2/g)
x: mass per unit area of paper (g/cm^2)
x_1: mass per unit area of ash (g/cm^2)

In the same batch of paper, (μ_1/ρ) and (μ_2/ρ) are constants, and x can be simply measured. By calculating the energy intensity logarithmic ratio using the model proposed in this study, polynomial fitting is applied to the relationship between the energy intensity logarithmic ratio and the mass attenuation coefficient. Substituting the results into Eq. 12 allows for the calculation of the ash content per unit area of the paper. By inputting the experimental measurement data into the model, this provides theoretical guidance for continuous X-ray measurement of quantitative paper ash content.

CONCLUSION

This study uses COMSOL software to establish an X-ray energy model for measuring paper ash content, examining the intensity attenuation of X-rays with an energy of 10 keV through four different material models: $CaCO_3$, TiO_2, wood plant fibers, and $CaCO_3$-filled paper samples. The model's accuracy is verified through theoretical analysis and experimental comparison. The simulation results show that the intensity attenuation of the $CaCO_3$-filled paper model aligns with experimental observations. The addition of fillers to the paper changes its density, light transmission, and other physical properties, validating the feasibility of using continuous X-rays to measure paper ash content and providing a deeper understanding of the energy conversion process of X-rays in paper.

Using the continuous X-ray method and the proposed model, the mass attenuation coefficients of paper samples with different ash contents of $CaCO_3$ and kaolin fillers were measured and calculated. At the same time, the experimental voltage logarithmic ratio was compared with the simulated energy intensity logarithmic ratio. The experimental results indicate that the energy model proposed for X-ray measurement of paper ash content can not only effectively measure the mass attenuation coefficient but it can also calculate the paper ash content. By inputting the data into the model to recalculate the attenuation coefficient and incorporating it into the experimental calculations, the model reduced the measurement error by 1%, significantly improving the reliability and accuracy of the measurements. **TJ**

ACKNOWLEDGEMENTS

This study was funded by the "Shaanxi Province 2023 Key Research and Development Program" (Project No. 2023-YBGY-331). The authors would like to thank 2023-YBGY-331 for their generous support of this study. At the same time, we would like to thank the Key Laboratory of Pulp and Paper Engineering, Shaanxi University of Science and Technology, for their support in this research.

LITERATURE CITED

1. Song, S., Qiang, S., Zhang, M., et al., *J. Shaanxi Univ. Sci. Technol.* 38(5): 6(2020).
2. Chauhan, V.S., Sharma, A., Chakrabarti, S.K., et al., *IPPTA* 23(3): 171(2011).
3. Shen, J., Song, Z., Qian, X., et al., *Ind. Eng. Chem. Res.* 50(2): 661(2011). https://doi.org/10.1021/ie1021078.
4. Hu, L., Lu, X., and Ma, J., *BioResources* 15(1): 2096(2020). https://doi.org/10.15376/biores.15.1.2096-2110.
5. Huang, M., *Nucl. Technol.* 13(4): 216(1990).
6. Ou, X.G., *Automation Instruments* 19(7): 7(1998).
7. Rozic, M., Macefat, M., and Orescanin, V., *Nucl. Instrum. Methods Phys. Res., Sect. B* 229(1): 117(2004). https://doi.org/10.1016/j.nimb.2004.11.011.
8. Lu, X.Y., "Study on the quantitative detection of total ash and its components in paper by continuous X-ray method," Master's thesis, Shaanxi University of Science and Technology, Xi'an, Shaanxi, China, 2021.
9. Zhang, Y., Huang, J., Hu, T., et al., *J. Beijing Norm. Univ., Nat. Sci.* 50(2): 139(2014).
10. Huang, K., Li, W., Xiong, T., et al., *Sci. Technol. Innov. Her.* 16(7): 162(2019).
11. Cao, Q. and Wang, Q., *Chinese J. Rad. Health* 22(6): 644(2013).
12. Li, Y., Yang, Z., and Wu, W., *Chin. J. Med. Phys.* 37(7): 850(2020).
13. Abdul Aziz, M.Z., Yani, S., Haryanto, F., et al., *J. Radiat. Res. Appl. Sci.* 13(1): 704(2020). https://doi.org/10.1080/16878507.2020.1828020.
14. Chao, Y., Xu, L., Hu, L., et al., *Chin. Phys. B* 29(9): 407(2020). https://doi.org/10.1088/1674-1056/aba2e4.
15. Osipov, S.P., Yadrenkin, I.G., Chakhlov, S.V., et al., *Russ. J. Nondestr. Test.* 57: 222(2021). https://doi.org/10.1134/S1061830921030049.
16. Chatterjee, S., Ghosh, S., and Mitra, D., *Nucl. Part. Phys., Proc.* 341: 1(2023). https://doi.org/10.1016/j.nuclphysbps.2023.09.005.
17. Wang, H., Liu, Q., Gu, C., et al., *Mechanical Engineer* 344(2): 114(2020).
18. Ren, X., *Internal Combustion Engine and Parts* 319(19): 82(2020).
19. He, S. and Wang, Y., *Chinese Medical Device Information* 28(7): 23,149(2022).
20. Guo, C. and Wu, Y., *Chin. Sci. Bull.* 30(11): 837(1985). https://doi.org/10.1360/csb1985-30-11-837.
21. Du, C., Xu, X., Zhao, H., *2008 Chinese Nuclear Society, Proceedings of the 14th National Academic Annual Conference on Nuclear Electronics and Nuclear Detection Technology* (lower volume), China, p. 6.
22. Zhang, L. and Dai, T., Modern Instrumentation 14(5): 50(2008).
23. Agarwal, B.K., *X-Ray Spectroscopy: An Introduction*, Springer Series in Optical Sciences, Springer-Verlag, Berlin, 1991.
24. Eisfeld, E. and Roth, J., *Adv. Opt. Technol.* 7(3): 189(2018). https://doi.org/10.1515/aot-2018-0005.

ABOUT THE AUTHORS

The existing methods for measuring paper ash content require significant human and material resources. Therefore, we approached these experiments from a simulation perspective, aiming to improve measurement accuracy while reducing costs. This study combines the continuous X-ray method for measuring paper ash content proposed by Lu [8], with experiments and simulations validating each other, aiming to improve measurement accuracy.

The most difficult part of this study was measuring the experimental data and establishing the paper ash content model. After reviewing relevant literature and conducting numerous repetitive experiments, these challenges were ultimately overcome.

Through this work, we found that simulation methods can effectively reduce systematic errors in the experimental process. It was surprising to see that by inputting the experimental data into the model, the experimental error could be effectively reduced to nearly 1%.

In pulp and paper mills, inputting various paper parameters into the model used here lets the model serve as a supportive foundation for subsequent experiments and validations. As a next step in this research, we plan to introduce a temperature variable in the simulation process, exploring the impact of temperature on the continuous X-ray method for measuring paper ash content, with the goal of proposing an appropriate temperature compensation formula.

Hu is associate professor and Chen is a Master's student in the College of Mechanical and Electrical Engineering at Shaanxi University of Science and Technology in Xi'an, Shaanxi, China. Email Chen at 220511042@sust.edu.cn.

Hu

Chen

25. Hubbell, J.H. and Seltzer, S.M., "Tables of X-ray mass attenuation coefficients and mass energy-absorption coefficients from 1 keV to 20 MeV for elements Z = 1 to 92 and 48 additional substances of dosimetric interest," in *X-Ray Mass Attenuation Coefficients: NIST Standard Reference Database 126*, National Institute of Standards and Technology, Gaithersburg, M, USA, 1995. Available [Online] http://physics.nist.gov/PhysRefData/XrayMassCoef/cover.html.
26. Ma, Y.Q., "X-ray biocrystal diffraction analysis of GaAs multilayer heteroepitaxial structured materials and SiC MESFET structured materials," Master's thesis, Hebei University of Technology, Tianjin, China, 2007.
27. Hu, L. and Lu, X., *Chem. Pap.* 75(11): 5861(2021). https://doi.org/10.1007/s11696-021-01764-y.

ABOUT THIS PAPER

Cite this article as:
Hu, L. and Chen, W., *TAPPI J.* 24(5): 266(2025). https://doi.org/10.32964/TJ24.5.266

DOI: https://doi.org/10.32964/TJ24.5.266

ISSN: 0734-1415

Publisher: TAPPI Press

About this journal